








RESEARCH

Open Access



Targeted next-generation sequencing for detection of *PIK3CA* mutations in archival tissues from patients with Klippel–Trenaunay syndrome in an Asian population

Yuki Sasaki^{1,2†}, Kosuke Ishikawa^{1,2*†}, Kanako C. Hatanaka³, Yumiko Oyamada⁴, Yusuke Sakuhara⁵, Tadashi Shimizu⁵, Tatsuro Saito^{6,7}, Naoki Murao², Tomohiro Onodera⁸, Takahiro Miura¹, Taku Maeda¹, Emi Funayama¹, Yutaka Hatanaka^{3,6}, Yuhei Yamamoto¹ and Satoru Sasaki²

Abstract

Background Klippel–Trenaunay syndrome (KTS) is a rare slow-flow combined vascular malformation with limb hypertrophy. KTS is thought to lie on the *PIK3CA*-related overgrowth spectrum, but reports are limited. *PIK3CA* encodes p110 α , a catalytic subunit of phosphatidylinositol 3-kinase (PI3K) that plays an essential role in the PI3K/AKT/mammalian target of rapamycin (mTOR) signaling pathway. We aimed to demonstrate the clinical utility of targeted next-generation sequencing (NGS) in identifying *PIK3CA* mosaicism in archival formalin-fixed paraffin-embedded (FFPE) tissues from patients with KTS.

Results Participants were 9 female and 5 male patients with KTS diagnosed as capillaro-venous malformation (CVM) or capillaro-lymphatico-venous malformation (CLVM). Median age at resection was 14 years (range, 5–57 years). Median archival period before DNA extraction from FFPE tissues was 5.4 years (range, 3–7 years). NGS-based sequencing of *PIK3CA* achieved an amplicon mean coverage of 119,000x. *PIK3CA* missense mutations were found in 12 of 14 patients (85.7%; 6/8 CVM and 6/6 CLVM), with 8 patients showing the hotspot variants E542K, E545K, H1047R, and H1047L. The non-hotspot *PIK3CA* variants C420R, Q546K, and Q546R were identified in 4 patients. Overall, the mean variant allele frequency for identified *PIK3CA* variants was 6.9% (range, 1.6–17.4%). All patients with geographic capillary malformation, histopathological lymphatic malformation or macrodactyly of the foot had *PIK3CA* variants. No genotype–phenotype association between hotspot and non-hotspot *PIK3CA* variants was found. Histologically, the vessels and adipose tissues of the lesions showed phosphorylation of the proteins in the PI3K/AKT/mTOR signaling pathway, including p-AKT, p-mTOR, and p-4EBP1.

[†]Yuki Sasaki and Kosuke Ishikawa have contributed equally to this work.

*Correspondence:
Kosuke Ishikawa
kishikawa-hok@umin.ac.jp

Full list of author information is available at the end of the article



© The Author(s) 2023, corrected publication 2024. **Open Access** This article is licensed under a Creative Commons Attribution 4.0 International License, which permits use, sharing, adaptation, distribution and reproduction in any medium or format, as long as you give appropriate credit to the original author(s) and the source, provide a link to the Creative Commons licence, and indicate if changes were made. The images or other third party material in this article are included in the article's Creative Commons licence, unless indicated otherwise in a credit line to the material. If material is not included in the article's Creative Commons licence and your intended use is not permitted by statutory regulation or exceeds the permitted use, you will need to obtain permission directly from the copyright holder. To view a copy of this licence, visit <http://creativecommons.org/licenses/by/4.0/>. The Creative Commons Public Domain Dedication waiver (<http://creativecommons.org/publicdomain/zero/1.0/>) applies to the data made available in this article, unless otherwise stated in a credit line to the data.

Conclusions The PI3K/AKT/mTOR pathway in mesenchymal tissues was activated in patients with KTS. Amplicon-based targeted NGS could identify low-level mosaicism from low-input DNA extracted from FFPE tissues, potentially providing a diagnostic option for personalized medicine with inhibitors of the PI3K/AKT/mTOR signaling pathway.

Keywords Capillary malformations, High-throughput nucleotide sequencing, Klippel–Trenaunay Syndrome, Limb hypertrophy, Lymphatic abnormalities, Phosphatidylinositol 3-Kinase, *PIK3CA*-related overgrowth spectrum, Segmental hypertrophy, Vascular malformations, Venous malformations

Background

Klippel–Trenaunay syndrome (KTS, [MIM 149,000]) is a slow-flow combined vascular malformation with a characteristic triad of symptoms: capillary malformation (CM), limb hypertrophy, and venous malformation (VM) with or without lymphatic malformation (LM) [1, 2]. From 2012 onward, several studies have reported on *PIK3CA* variants found in KTS. Kurek et al. screened DNA extracted from lesional tissue in 3 of 15 patients with KTS and found *PIK3CA* variants [3]. Luks et al. reported that up to 90% of patients with KTS have *PIK3CA* variants in pathological lesions. Accordingly, KTS is thought to lie on the *PIK3CA*-related overgrowth spectrum (PROS) [4, 5], but reports are limited [3, 6–9] and genetic differences among races are unknown.

PIK3CA encodes p110 α , a catalytic subunit of phosphatidylinositol 3-kinase (PI3K) that plays a role in cellular processes such as proliferation, motility, invasion, and death through its involvement in the PI3K/AKT/mammalian target of rapamycin (mTOR) signaling pathway [10]. Moreover, p110 α is required for endothelial cell migration during angiogenesis [11, 12], and its aberrant activation has been associated with the development of vascular malformations [13, 14]. Activation of PI3K leads to phosphorylation of AKT followed by mTOR and its downstream targets, including eukaryotic translation initiation factor 4E-binding protein 1 (4EBP1) [15].

The activation of mutations in *PIK3CA* is reported to play a role in many human cancers [16]. Of the *PIK3CA* variants, more than 80% are found at three hotspots: the glutamates E542 and E545, located in the helical domain of exon 10, and the histidine H1047, located in the kinase domain of exon 21 [17]. These three mutations exert the strongest effect on downstream signaling and enzymatic activation [17]. In patients with KTS as well, E542K, E545K, H1047R, and H1047L are the most frequent (i.e., hotspot) variants [3, 6, 8, 9].

These somatic gain-of-function variants, which arise in the postzygotic stage during embryonic development, result in a mosaic pattern in the affected lesion [5]. Therefore, molecular testing of peripheral blood or saliva has been ineffective for detecting pathogenic variants in patients with PROS [3]. Meanwhile, archival formalin-fixed paraffin-embedded (FFPE) tissues can be a valuable resource for clinical genomic studies [18], but the DNA obtained from these tissues can have a wide range of

quality depending on factors such as age, DNA–protein crosslinking, fixation conditions, and inhibitors, all of which can affect downstream genomic analyses [19].

Next-generation sequencing (NGS) involving an amplicon-based targeted sequencing method with high sensitivity can identify low-level mosaicism from low-input DNA extracted from FFPE tissues and provide a diagnostic option when affected tissue is available [20]. Therefore, this study aimed to demonstrate the clinical utility of targeted NGS with a custom-designed panel for identifying *PIK3CA* mosaicism in archival FFPE tissues from patients with KTS, a relatively rare vascular malformation with limb hypertrophy.

Results

Patient characteristics

Participants were 9 female and 5 male patients, including 5 (35.7%) adults (defined as age 18 years or older). Their clinical characteristics and genetic profiles are shown in Table 1. Median age at resection was 14 years (range, 5–57 years). Archival median period before DNA extraction from FFPE tissues was 5.4 years (range, 3–7 years). Lesions were resected from the abdomen ($n=2$), buttock ($n=1$), thigh ($n=2$), knee ($n=3$), lower leg ($n=4$), and foot ($n=2$). Tissue specimens were skin with subcutaneous tissue ($n=8$), subcutaneous tissue only ($n=5$), and subcutaneous tissue with muscles ($n=1$). Figure 1 shows clinical photographs and magnetic resonance imaging (MRI) of all patients with detected *PIK3CA* variants. Patient 1 [21], patients 3 and 4 [22], and patient 9 [23] were previously reported without genetic analyses.

Clinicopathological diagnoses were capillaro-venous malformation (CVM) ($n=8$) and capillaro-lymphatico-venous malformation (CLVM) ($n=6$). Geographic CMs were found in 8 patients. Lower limb discrepancy (LLD) in terms of length was found in 7 patients, including 2 patients with epiphysiodesis, while LLD in terms of girth was observed in all 14 patients (right-sided hypertrophy in 7 patients). Digital anomalies were found in 5 patients as macrodactyly of the foot. Patient 7 had bilateral lesions in the lower limbs (with CLVM in the left limb) and bilateral macrodactyly, and the longer right limb required epiphysiodesis. Thirteen patients had received treatment prior to resection for genetic analysis, including partial resection ($n=10$), percutaneous sclerotherapy ($n=12$), transcatheter arterial embolization for

Table 1 Summary of clinical manifestations and identified *PIK3CA* variants in patients with Klippel–Trenaunay syndrome

Patient	Sex	Age (years)*	Lesions resected	Specimen	Identified variants	VAF	Diagnoses	Types of CM	Lower limb discrepancy in		Macroductyly	Previous treatments
									Length	Girth		
1	M	36	Thigh	Skin, SC	C420R	1.6%	CLVM	Geographic	—	Rt > Lt	Rt	PR, Sc
2	F	14	Abdomen	Skin, SC	E542K	3.3%	CLVM	—	—	Rt > Lt	—	PR, Sc, TAE
3	F	57	Lower leg	Skin, SC	E542K	10.9%	CVM	Geographic	Lt > Rt	Lt > Rt	Lt	PR, Sc
4	F	6	Knee	Skin, SC	E545K	7.5%	CLVM	Geographic	Lt (ED) > Rt	Lt > Rt	Lt	PR, HL, Sc, TAE
5	F	16	Abdomen	SC	E545K	12.7%	CLVM	Geographic	—	Lt > Rt	—	PR, Sc, TAE
6	M	7	Lower leg	SC	Q546R	3.9%	CLVM	Geographic	Rt (ED) > Lt	Lt > Rt	Bilateral	PR, HL, Sc
7	F	26	Foot	SC	Q546R	5.9%	CVM	Geographic	Rt > Lt	Rt > Lt	—	HL, Sc
8	M	25	Foot	SC	Q546K	2.3%	CVM	—	—	Rt > Lt	—	Sc
9	F	17	Knee	Skin, SC	H1047R	17.4%	CVM	Geographic	Rt > Lt	Rt > Lt	—	PR, Sc, TAE
10	F	5	Knee	Skin, SC	H1047R	1.6%	CVM	—	—	Rt > Lt	—	—
11	F	22	Thigh	SC, M	H1047R	8.1%	CVM	—	—	Lt > Rt	—	PR, Sc
12	M	11	Buttock	Skin, SC	H1047L	7.8%	CLVM	Geographic	Lt > Rt	Lt > Rt	Lt	PR, Sc, TAE
13	F	13	Lower leg	SC	—	—	CVM	—	—	Rt > Lt	—	HL, Sc, TAE
14	M	11	Lower leg	Skin, SC	—	—	CVM	—	—	Lt > Rt	—	PR, Sc

*Age at resection; SC, subcutaneous tissue; M, muscle; VAF, variant allele frequency; CM, capillary malformation; CVM, capillary venous malformation; CLVM, capillary-lymphatico-venous malformation; Lt, left; Rt, right; ED, epiphysiodesis; PR, partial resection; Sc, sclerotherapy; TAE, transcatheter arterial embolization; HL, high ligation of a lateral marginal vein in the thigh

micro-arteriovenous shunts ($n=6$), and high ligation of a lateral marginal vein in the thigh ($n=4$).

Detection of *PIK3CA* variants

Median DNA concentration from FFPE tissues measured using a Qubit 3.0 Fluorometer and a 2200 TapeStation system were respectively 20.5 ng/μL and 25.5 ng/μL. NGS-based ultradeep sequencing of *PIK3CA* achieved an amplicon mean coverage of 119,000x (range, 96,000–142,000x) for FFPE tissues and 107,000x (range, 95,000–136,000x) for controls.

The detected *PIK3CA* variant frequency in positive control DNA of 5%, 1%, 0.5%, and 0.1% of E545K/H1047R mixture were respectively 4.3%, 0.8%, 0.5%, and 0.1% in E545K and 10.3%, 1.2%, 0.5%, and 0.1% in H1047R. No *PIK3CA* variants were detected in negative control DNA. *PIK3CA* missense mutations were found in 12 of 14 patients (85.7%; 6/8 CVM and 6/6 CLVM) (Table 1). Of the 12 variants detected, 8 (66.7%) were hotspot variants: E542K (c.1624G>A) in 2 patients, E545K (c.1633G>A) in 2, H1047R (c.3140 A>G) in 3, and H1047L (c.3140 A>T) in 1. The rest were 3 distinct non-hotspot variants: C420R (c.1258T>C) in 1 patient, Q546R (c.1637 A>G) in 2, and Q546K (c.1636 C>A) in 1. All of the detected *PIK3CA* variants were previously reported in patients with PROS or LM and are considered pathogenic variants according to ClinVar (Table 2). Overall, the mean variant allele frequency (VAF) for the identified *PIK3CA* variants was 6.9% (range, 1.6–17.4%). Summaries of the *PIK3CA* variants in PROS ($n=696$) [3, 6–8, 20, 24–48] and vascular malformations except PROS (including LM, VM, fibro-adipose vascular anomaly and combined vascular malformations; $n=307$) [6, 8, 42, 49–55] from the literature as well as our cohort ($n=12$) are presented in Additional file 1, Fig. 2 (frequent variants in PROS ≥ 5 patients in each variant, $n=597$ from the literature; vascular malformations except PROS, $n=300$), and Table 2 (variants presented in Fig. 2), including the ranks in COSMIC v97 and variant class in ClinVar.

Genotype–phenotype analysis

All patients with geographic CM, histopathological LM, or macroductyly of the foot had *PIK3CA* variants. However, we did not find any association with phenotype or its severity between hotspot and non-hotspot *PIK3CA* variants.

Histopathological analysis

The expression of D2-40 in lymphatic endothelial cells was confirmed in 6 patients. Anastomosing vascular channels were found in all 14 patients with positive stains for p-AKT ($n=12$), p-mTOR ($n=7$), and p-4EBP1 ($n=14$); small vessels were found in 11 patients with positive stains for p-AKT ($n=10$), p-mTOR ($n=1$), and p-4EBP1

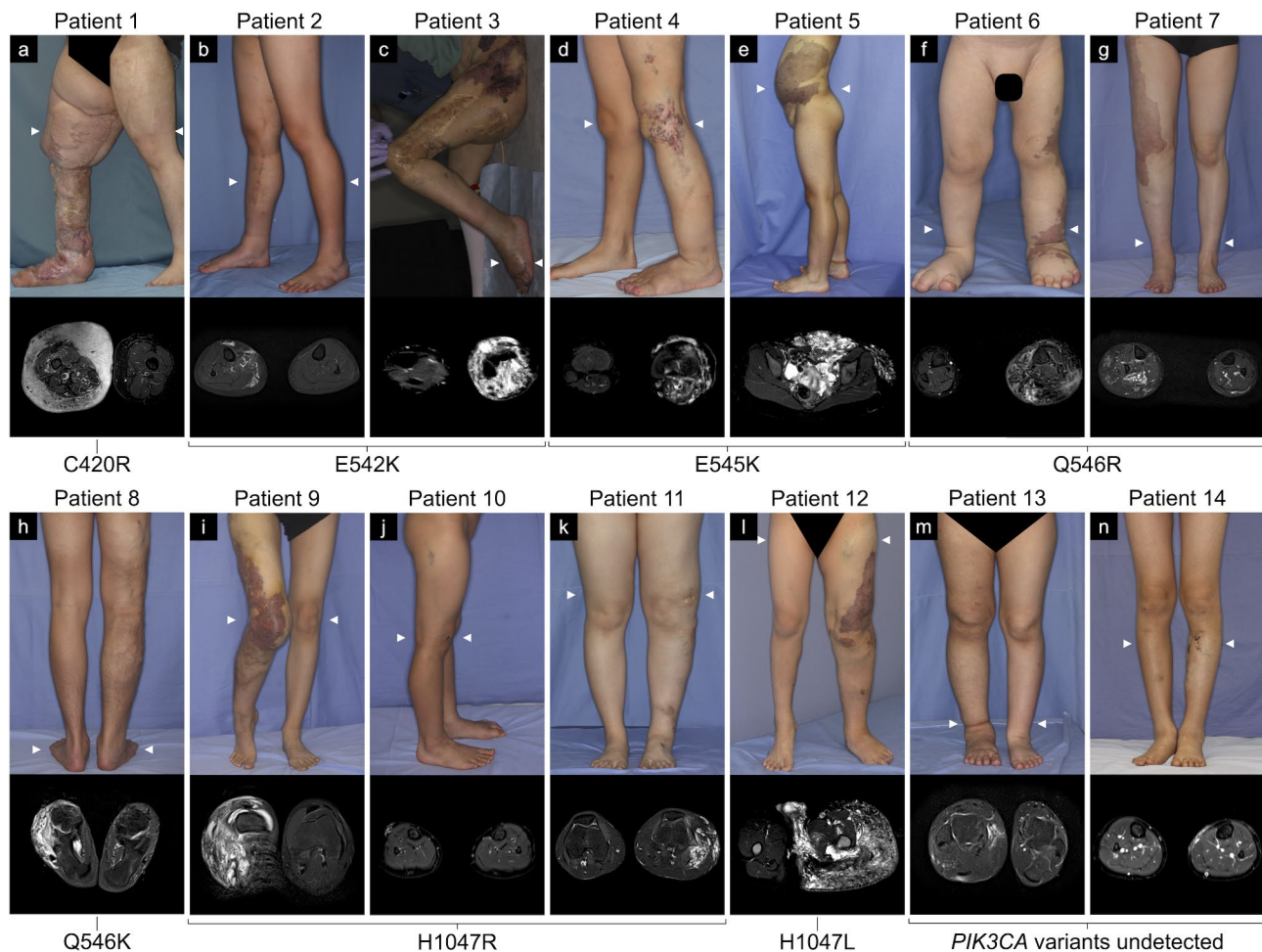


Fig. 1 Clinical photographs (upper) and short-tau inversion recovery or fat-suppressed T2-weighted magnetic resonance images (lower) of the patients with Klippel-Trenaunay syndrome with detected or undetected *PIK3CA* variants. Various clinical manifestations were observed, including geographic capillary malformations (a, c-g, i, l), lower limb discrepancy in terms of length (c, d, f, g, i, l, m), and macrodactyly (a, c, d, f, l). Magnetic resonance images are axial views at the arrowhead position in each clinical photograph with the lesions of high signal intensity

($n=11$); venules were found in all 14 patients with positive stains for p-AKT ($n=14$), p-mTOR ($n=10$), and p-4EBP1 ($n=14$); and adipose tissues were found in all 14 patients with positive stains for p-AKT ($n=8$), p-mTOR ($n=1$), and p-4EBP1 ($n=12$). Positive stains for p-AKT, p-mTOR, and p-4EBP1 were also found in two patients with undetected *PIK3CA* variants in vessels and adipose tissues. Representative images of hematoxylin and eosin, p-AKT, p-mTOR, and p-4EBP1 stains are shown in Fig. 3. The immunohistochemical analysis results for all patients are shown in Table 3.

Discussion

This study investigated the largest cohort of molecularly diagnosed patients with KTS in an Asian population. Using archival FFPE tissues, we identified *PIK3CA* variants in 85.7% of our cohort with KTS, 66.6% of which were the hotspot variants E542K, E545K, H1047R, and H1047L. The non-hotspot variants Q546K and Q546R

were also identified, despite being rare in patients with vascular malformations. To our knowledge, Q546K was previously unreported in patients with KTS but was found in a patient with a fibro-adipose vascular anomaly [6] and in 3 patients with LM [8, 52]. Q546R has been reported in a patient with KTS [7] as well as a patient with LM [8] (Fig. 2). Our mutational findings were in line with those of patients with KTS in Western populations [3, 6, 8].

The PI3K catalytic subunit p110 α encoded by *PIK3CA* has five domains: a C2 domain, a helical domain, a kinase domain, an N-terminal adapter-binding domain, and a Ras-binding domain (Fig. 2) [56]. In many cancers, mutations are found throughout the entire p110 α protein, except for the Ras-binding domain, including the following hotspots: E542 and E545 in the helical domain and H1047 in the kinase domain [17]. The *PIK3CA* variants in PROS, including KTS, have a similar profile to that in cancers (Table 2), and an association of hotspot variants

Table 2 Summary of the frequent *PIK3CA* variants found in PROS and vascular malformations

Amino acid variants	Ranks in COSMIC ¹	Counts ¹	Relative frequency ²	Variant class ³
H1047R ^a	1	5,368	36.73	Pathogenic
E545K ^a	2	4,111	28.13	Pathogenic
E542K ^a	3	2,515	17.21	Pathogenic
H1047L ^a	4	739	5.06	Pathogenic
Q546K ^b	8	301	2.06	Conflicting interpretations of pathogenicity
C420R ^b	9	258	1.77	Pathogenic
M1043I	11	190	1.30	Pathogenic/Likely pathogenic
E726K	12	168	1.15	Pathogenic
Q546R ^b	13	150	1.03	Pathogenic
H1047Y	14	143	0.98	Pathogenic
G118D	15	124	0.85	Pathogenic
E81K	17	113	0.77	Pathogenic
E453K	19	98	0.67	Pathogenic
Y1021C	25	77	0.53	Pathogenic
T1025A	31	60	0.41	Pathogenic/Likely pathogenic
E545D	34	58	0.40	Pathogenic/Likely pathogenic
E110del	42	46	0.31	Likely pathogenic
E365K	54	34	0.23	Pathogenic
P104L	63	26	0.18	Pathogenic/Likely pathogenic
A1035V	113	11	0.08	Pathogenic
G914R	127	9	0.06	Pathogenic
R115P	159	6	0.04	Likely pathogenic
C378Y	159	6	0.04	Pathogenic
E453del	177	5	0.03	Pathogenic
Total <i>PIK3CA</i> variants		14,616	100	

The *PIK3CA* variants found in *PIK3CA*-related overgrowth spectrum (PROS) [3, 6–8, 20, 24–48] and vascular malformations [6, 8, 42, 49–55]. ^aHotspot variants. ^bNon-hotspot variants detected in our cohort. ¹Ranks and counts in COSMIC (Catalogue of Somatic Mutations in Cancer) v97. ²Relative frequency in this table. ³Variant class in ClinVar.

with more severe hypertrophy has been suggested, with milder hypertrophy linked to rarer non-hotspot variants [7, 27, 30]. However, in our cohort, patients who had non-hotspot variants did not exhibit milder hypertrophy compared with those who had hotspot variants. Thus, a meta-analysis should be conducted to clarify any potential genotype–phenotype correlations in this rare disease. To that end, molecular diagnoses may prove helpful in providing prognostic information on clinical manifestations [20].

Molecular genetic testing for the diagnosis of PROS requires clinically affected tissues, preferably fresh frozen tissues [4]. Testing can be performed using FFPE tissues; however, unlike fresh frozen tissues, DNA obtained from FFPE tissues can vary widely in terms of quality [19]. NGS with the use of a highly sensitive amplicon-based

targeted sequencing method can identify low-level mosaicism from DNA extracted from widely available archival FFPE tissues [20]. Although digital droplet PCR is a simple and highly sensitive and specific method for the detection and quantification of targeted DNA variants, entire exons must be sequenced by NGS in order to capture all the coding single-nucleotide variants as well as small insertion and deletion variants in rare diseases [4]. Detection of rare variants remains a challenge because of the error-prone nucleotide changes resulting from sequencing errors. NGS combined with molecular barcodes can eliminate false-positive variants and enable detection thresholds of 0.1% VAF [57].

Using archival FFPE tissues, we were able to compare the genotype and histology of the lesions. Immunohistochemistry revealed that the vessels in all 14 patients and the adipose tissues in 13 patients expressed p-AKT, p-mTOR, and/or p-4EBP1 (Fig. 3; Table 3), indicating enhanced activation of the PI3K/AKT/mTOR pathway in mesenchymal tissues compared with that in normal tissues in these patients with KTS. These findings are in line with previous reports of *PIK3CA* variants detected in adipocytes in PROS [3] and abnormal vessels detected in fibro-adipose vascular anomaly [58]. However, 2 patients (patients 13 and 14) with undetected *PIK3CA* variants showed some expression of p-AKT, p-mTOR, and/or p-4EBP1 in vessels and adipose tissues. Neither had geographic CM, histopathological LM, or macrodactyly of the foot. Patient 13 can be diagnosed with CVM and congenital nonprogressive limb overgrowth [59] caused by somatic *GNAI1* mutation [60]. Patient 14 might have common VM caused by a somatic *TEK* mutation [61] encoding TIE2 upstream of the PI3K/AKT/mTOR pathway.

To date, fewer than 30 different *PIK3CA* gene variants have been reported in PROS, five of which—C420R, E542K, E545K, H1047R, and H1047L—have been shown to be recurrent [5]. As for the *PIK3CA* variants in patients with KTS [3, 6–9], Kurek et al. reported H1047R in 3 of 15 patients [3], while Luks et al. reported E542K in 3, E545K in 9, E545G in 1, H1047R in 6, and H1047L in 1 of 21 patients [6]. Kuentz et al. reported G364R in 1, E542K in 1, E545K in 2, Q546R in 1, and H1047L in 1 of 13 patients [7]. Brouillard et al. reported E110del in 1, and E545K in 3 of 4 patients [8]. Nozawa et al. reported E542K in 2, E545K in 5, and H1047R in 1 of 10 patients [9].

The theascreen® PIK3CA RGQ PCR Kit was developed to be a companion diagnostic tool for 11 *PIK3CA* gene variants: C420R, E542K, E545A, E545D, E545G, E545K, Q546E, Q546R, H1047L, H1047R, and H1047Y. It uses genomic DNA extracted from FFPE or circulating tumor DNA isolated from plasma in patients with breast cancer. Patients with advanced or metastatic breast cancer who

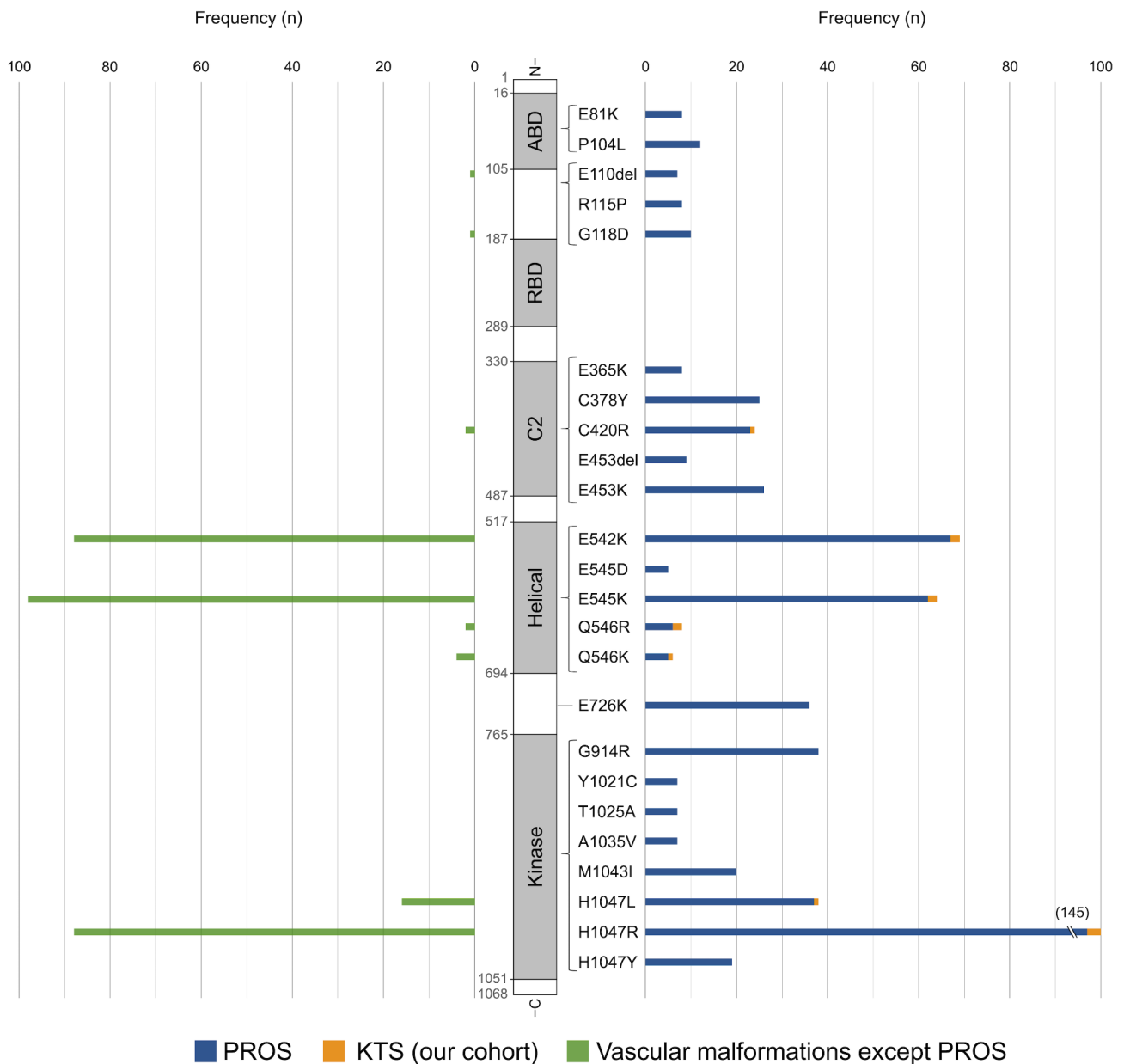


Fig. 2 Distribution of frequent *PIK3CA* variants in *PIK3CA*-related overgrowth spectrum (PROS) [3, 6–8, 20, 24–48] and vascular malformations [6, 8, 42, 49–55] from the literature as well as our cohort (variants in PROS ≥ 5 patients in each variant). Right, variants found in patients with PROS (blue, n = 597) in the literature and Klippel–Trenaunay syndrome (KTS) in our cohort (orange, n = 12). Left, variants found in patients with vascular malformations except PROS (green, n = 300) in the literature. ABD, p85α-binding domain; RBD, Ras-binding domain; C2, C2 domain; Helical, helical domain; Kinase, kinase domain

test positive for the presence of one or more *PIK3CA* variants are eligible for treatment with the PI3K inhibitor alpelisib [62]. With a limit of detection from 2.4 to 14.04% VAF [63], the thescreen kit would not have detected five cases in our cohort because of the low VAF (C420R with 1.6% VAF; E542K with 3.3% VAF; Q546R with 3.9% VAF and 5.9% VAF, respectively; and H1047R with 1.6% VAF) as well as one case with the Q546K variant, which is not targeted by the kit.

Our findings have potential implications for the treatment of patients with KTS using inhibitors of the PI3K/

AKT/mTOR signaling pathway, which have shown promising results with mTOR inhibitor sirolimus [64, 65], pan-AKT inhibitor miransertib [66], and selective class I PI3K inhibitor alpelisib [67] or taselisib [68]. It is thus critical to obtain more detailed information regarding specific variants in order to identify of the options for targeted treatment [69].

This study has some limitations. First, we evaluated only patients with KTS who were diagnosed based on the triad of CM, VM, and hypertrophy of the affected limb [2], so there was no controlling for vascular

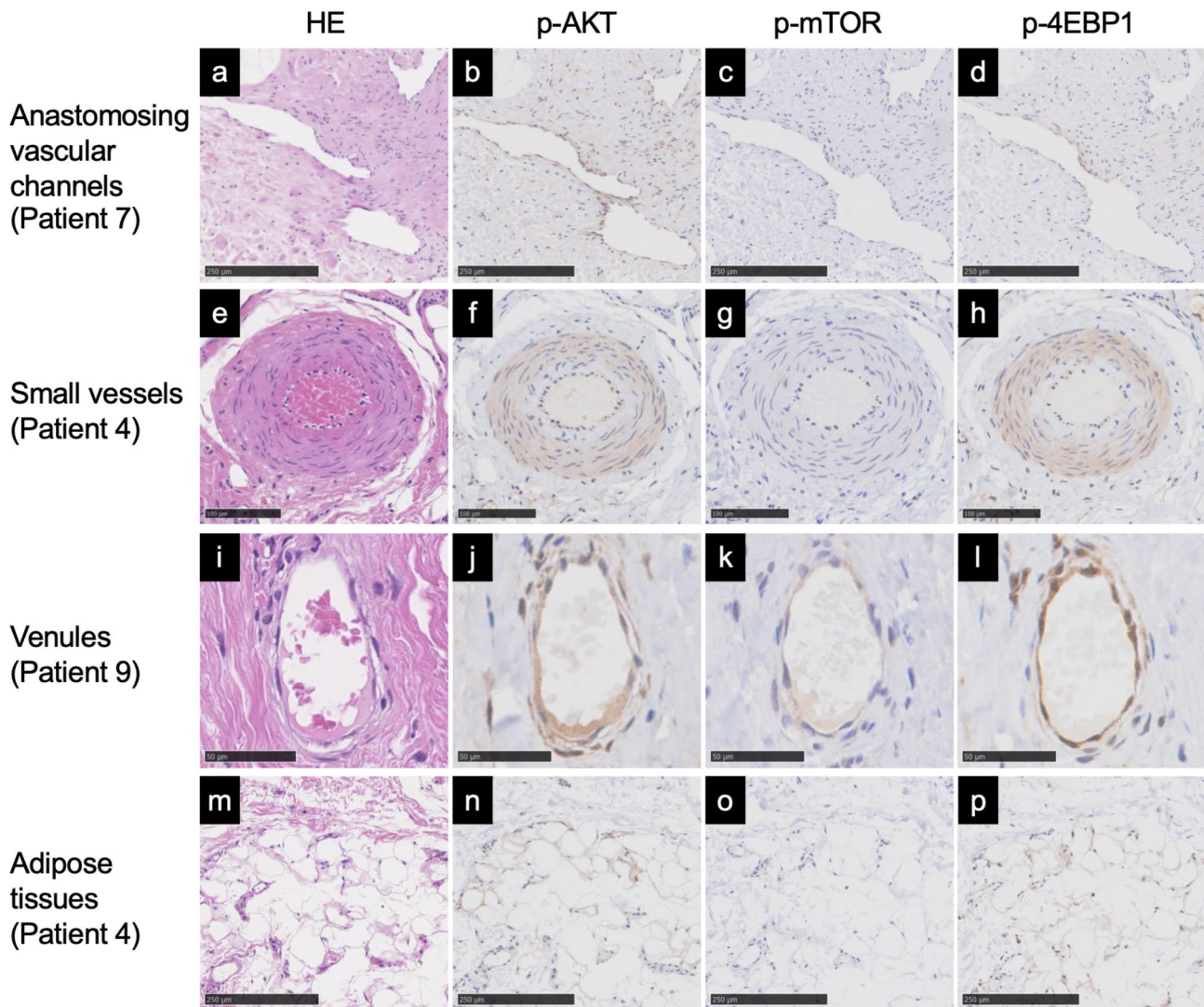


Fig. 3 Histology and immunohistochemical analysis of the PI3K/AKT/mTOR signaling pathway in the serial sections of patients with Klippel-Trenaunay syndrome. Representative images of anastomosing vascular channels (a-d), small vessels (0.1–1.0 mm diameter) (e-h), venules (10–100 μm diameter) (i-l), and adipose tissues (m-p). Staining for hematoxylin and eosin (HE) (a, e, i, m), p-AKT (b, f, j, n), p-mTOR (c, g, k, o), and p-4EBP1 (d, h, l, p). Cytoplasmic intensity of the immunohistochemical stains graded as positive (b, d, f, h, j, k, l, n, p) and negative (c, g, o). Scale bars: a-d, m-p = 250 μm, e-h = 100 μm, i-l = 50 μm

malformations except KTS in the immunohistochemical analysis. Second, we performed targeted sequencing of *PIK3CA* gene coding sequences using a panel consisting of amplicons with an overall coverage of 87.9%, so genes not on the panel would have been missed.

Conclusions

We identified *PIK3CA* variants in 12 of 14 patients (85.7%) with KTS by using archival FFPE tissues, and 8 of these patients had the following hotspot variants: E542K, E545K, H1047R, and H1047L. The rarer non-hotspot *PIK3CA* variants Q546R and Q546K were also identified in 3 patients. Amplicon-based targeted NGS was able to identify low-level mosaicism from low-input DNA

extracted from FFPE tissues, suggesting its potential as a diagnostic option for personalized medicine.

Methods

Patients

This retrospective study involved Japanese patients with vascular malformations with lower limb hypertrophy who underwent resection of the vascular malformations at Tonan Hospital between 2011 and 2020. Of the 17 patients identified, 14 provided written informed consent and were included in the analysis. KTS was diagnosed based upon the triad of CM, VM, and hypertrophy of the affected limb [2]. In younger patients, VM was often less

Table 3 Immunohistochemical analysis of the lymphatic endothelial marker D2-40 and the PI3K/AKT/mTOR signaling pathway

Patient	D2-40	Anastomosing vascular channels				Small vessels				Venules				Adipose tissues			
		p-AKT	p-mTOR	p-4EBP1	p-AKT	p-mTOR	p-4EBP1	p-AKT	p-mTOR	p-4EBP1	p-AKT	p-mTOR	p-4EBP1	p-AKT	p-mTOR	p-4EBP1	
1	+	+	-	+	+	-	+	+	+	+	+	+	+	+	+	+	
2	+	-	+	+	+	-	+	+	+	+	+	+	+	-	+	+	
3	-	+	+	+	+	-	+	+	+	+	+	+	+	-	+	+	
4	+	-	+	+	+	-	+	+	+	+	+	+	+	-	+	+	
5	+	-	+	+	+	-	+	+	+	+	+	+	+	-	+	+	
6	+	+	+	+	None	None	None	None	None	None	None	None	None	+	+	-	
7	-	+	+	+	+	+	+	+	+	+	+	+	+	-	+	+	
8	-	+	+	+	+	-	+	+	+	+	+	+	+	-	+	+	
9	-	+	+	+	+	-	+	+	+	+	+	+	+	-	+	+	
10	-	+	+	+	None	None	None	None	None	None	None	None	None	+	+	+	
11	-	-	+	+	+	-	+	+	+	+	+	+	+	-	+	+	
12	+	-	+	+	-	-	+	+	+	+	+	+	+	-	+	+	
13	-	-	+	+	+	-	+	+	+	+	+	+	+	-	+	+	
14	-	-	+	+	None	None	None	None	None	None	None	None	None	+	+	+	

The expression of D2-40 in lymphatic endothelial cells was graded as positive (+) or negative (-). The cytoplasmic intensity of the immunohistochemical stains was graded as positive (+) or negative (-) in p-AKT, p-mTOR, and p-4EBP1. None, no small vessels observed

conspicuous but was diagnosed based on veins that were subtly dilated relative to the unaffected limb [70].

The patients' medical charts were reviewed, and the following demographic information and medical history data were collected: sex, date and age at resection, lesion resected, type of tissues in resected specimens, clinical photographs, and radiologic studies. Geographic CMs were defined as those with sharply demarcated borders and saturated dark red/purple color throughout the entire stain [70].

Prior to resection, all patients underwent MRI and color duplex ultrasound to evaluate the characteristics, distribution, and extent of the lesions. Vascular malformations were diagnosed based on the clinical history as well as the physical examination, ultrasonography, and MRI findings. LLD was evaluated in terms of length and girth according to teleoroentgenography and cross-section on MRI, respectively. LLD in terms of length was defined as 5 mm longer compared with the unaffected limb in children and 1 cm longer in adults, while LLD in terms of girth was defined as 10% greater in cross-sectional area compared with the unaffected limb [71].

DNA extraction

Surgical specimens were fixed with 10% buffered formalin and embedded in paraffin. Affected tissue was retrieved from archived FFPE tissue blocks. QIAamp DNA FFPE Tissue Kit (Qiagen, Germantown, MD) was used to extract genomic DNA from FFPE tissues. The positive and negative control DNA from the FFPE *PIK3CA* Reference Standard (E545K, HD112; H1047R, HD599; wild-type [WT], HD320; Horizon Discovery, Cambridge, UK) were extracted using a Maxwell RSC FFPE DNA Kit (Promega, Madison, WI). The concentration and quality of the extracted DNA were assessed using a 2200 TapeStation system with the Genomic DNA ScreenTape (Agilent, Santa Clara, CA) and a Qubit 3.0 Fluorometer with a Qubit dsDNA BR Assay Kit (Thermo Fisher Scientific, Waltham, MA), respectively. DNA controls were prepared for each condition: 5%, 1%, 0.5% and 0.1% of E545K/ H1047R mixture diluted in WT for the positive controls and only WT for the negative control.

Next-generation sequencing

We used an Ion AmpliSeq™ HD Made-to-Order Panel (IAH215884_374) to perform targeted sequencing of all *PIK3CA* gene coding sequences (3,607 bp). The panel consisted of 64 amplicons with an overall coverage of 87.9%. Deaminated cytosine residues were removed from 20 ng of the sample DNA and the target region was amplified using multiplex PCR with the Ion AmpliSeq™ HD Library Kit (Thermo Fisher Scientific). The primer sequence in the amplicon was partially digested, and the library was amplified using primers, to which barcode

sequences were added using Ion AmpliSeq™ HD Dual Barcode Kit (Thermo Fisher Scientific). After purification of the library DNA, the concentration and size of DNA were checked, and the library was mixed. Emulsion PCR was performed to clonally amplify the library DNA on beads and then template beads were collected and sequencing reactions were performed on the Ion S5™ XL system (Thermo Fisher Scientific) using an Ion Chef 550 Chip Kit (Thermo Fisher Scientific).

Bioinformatics analysis for detection of *PIK3CA* variant

The quality of the read data was checked, and the adapter sequences and poor-quality reads were removed. Then, the reads were mapped to reference sequences (hg19) using the torrent mapping alignment program of Torrent Suite ver. 5.16.1 (Thermo Fisher Scientific) and variants were detected using Ion Reporter ver. 5.18 (Thermo Fisher Scientific). Annotation information was assigned to the detected variants. The thresholds for the main parameters of Ion Reporter's variant detection were set as follows: Downsample to Coverage: 20,000; Minimum Allele Frequency of SNP (single nucleotide polymorphism), MNP (multiple nucleotide polymorphism), and INDEL (insertion or deletion of nucleotides): 0.05%; Minimum Variant Score of SNP and MNP: 6; Minimum Variant Score of INDEL: 10.

Histology and immunohistochemistry

The serial FFPE Sect. (5 μm thick) were stained using immunohistochemical as well as hematoxylin and eosin stains for a lymphatic endothelial marker D2-40 (#916,606, 1:1,000, BioLegend, San Diego, CA), p-AKT (#4060, 1:75; Cell Signaling Technology, Danvers, MA), p-mTOR (#2976, 1:100; Cell Signaling Technology), and p-4EBP1 (#2855, 1:200; Cell Signaling Technology). The expression of D2-40 in endothelial cells was used to diagnose LM. Vessels were categorized into three groups according to type and/or size: anastomosing vascular channels [72], small vessels (0.1–1.0 mm diameter), and venules (10–100 μm diameter). Vessels and adipose tissues were evaluated in terms of the cytoplasmic intensity of immunohistochemical stains graded as positive or negative by two independent observers. The connective tissues surrounding the lesions were used as a control.

Abbreviations

CM	capillary malformation
CVM	capillaro-venous malformation
CLVM	capillaro-lymphatico-venous malformation
4EBP1	eukaryotic translation initiation factor 4E-binding protein 1
FFPE	formalin-fixed paraffin-embedded
KTS	Klippel–Trenaunay syndrome
LLD	lower limb discrepancy
LM	lymphatic malformation
MRI	magnetic resonance imaging
mTOR	mammalian target of rapamycin
NGS	next-generation sequencing

PI3K	phosphatidylinositol 3-kinase
PROS	<i>PIK3CA</i> -related overgrowth spectrum
VAF	variant allele frequency
VM	venous malformation
WT	wild-type

Supplementary Information

The online version contains supplementary material available at <https://doi.org/10.1186/s13023-023-02893-1>.

Supplementary Material 1

Acknowledgements

We are grateful to all the patients for their invaluable participation. The authors thank Mayumi Shitamichi and the staff of the Clinical Biobank, Clinical Research and Medical Innovation Center, Hokkaido University Hospital, for technical assistance with the DNA extractions.

Authors' contributions

YS and KI analyzed the results and drafted the manuscript. KI and SS designed and coordinated the study. SS, NM, and TO were involved in recruiting patients. KCH and YO performed the histological analyses. YS and TSh performed the radiological analyses. YH and TS performed NGS and interpreted the genomic data. TMI, TM, EF, and YY revised the manuscript. All authors read and approved the final manuscript.

Funding

This study was supported in part by JSPS KAKENHI (JP18K16974) and a research grant from the Japan Intractable Diseases (Nanbyo) Research Foundation (2020B03).

Data Availability

The datasets generated and analyzed during this study are available from the corresponding author upon reasonable request.

Declarations

Ethics approval and consent to participate

The study was approved by the institutional review boards of Hokkaido University Hospital (number 016–0314) and Tonan Hospital (number 512) and was conducted in accordance with principles of the Declaration of Helsinki and its later amendments. The patients or their legal guardians gave their informed consent to be included.

Consent for publication

The patients or their legal guardians provided written informed consent for the publication of this study.

Competing interests

The authors declare no conflicts of interest.

Author details

¹Department of Plastic and Reconstructive Surgery, Faculty of Medicine, Graduate School of Medicine, Hokkaido University, Kita 15, Nishi 7, Kita-ku, Sapporo 060-8638, Japan

²Center for Vascular Anomalies, Department of Plastic and Reconstructive Surgery, Tonan Hospital, Hokkaido, Japan

³Center for Development of Advanced Diagnostics, Institute of Health Science Innovation for Medical Care, Hokkaido University Hospital, Hokkaido, Japan

⁴Department of Diagnostic Pathology, Tonan Hospital, Hokkaido, Japan

⁵Department of Diagnostic and Interventional Radiology, Tonan Hospital, Hokkaido, Japan

⁶Research Division of Genome Companion Diagnostics, Hokkaido University Hospital, Hokkaido, Japan

⁷Riken Genesis Co., Ltd, Tokyo, Japan

⁸Department of Orthopedic Surgery, Faculty of Medicine, Graduate School of Medicine, Hokkaido University, Hokkaido, Japan

Received: 19 April 2023 / Accepted: 26 August 2023

Published online: 04 September 2023

References

1. Klippel M, Trenaunay P. Mémoires originaux: du naevus variqueux osteo-hypertrophique. *Arch Gen Med (Paris)*. 1900;3:641–72.
2. ISSVA Classification of Vascular Anomalies. ©2018 International Society for the study of vascular anomalies available at issva.org/classification Accessed April 10, 2023.
3. Kurek KC, Luks VL, Ayturk UM, Alomari AI, Fishman SJ, Spencer SA, et al. Somatic mosaic activating mutations in *PIK3CA* cause CLOVES syndrome. *Am J Hum Genet*. 2012;90:1108–15. <https://doi.org/10.1016/j.ajhg.2012.05.006>.
4. Keppler-Noreuil KM, Rios JJ, Parker VE, Semple RK, Lindhurst MJ, Sapp JC, et al. *PIK3CA*-related overgrowth spectrum (PROS): diagnostic and testing eligibility criteria, differential diagnosis, and evaluation. *Am J Med Genet Part A*. 2015;167A:287–95. <https://doi.org/10.1002/ajmg.a.36836>.
5. Vahidnezhad H, Youssefian L, Uitto J. Klippel-Trenaunay syndrome belongs to the *PIK3CA*-related overgrowth spectrum (PROS). *Exp Dermatol*. 2016;25:17–9. <https://doi.org/10.1111/exd.12826>.
6. Luks VL, Kamitaki N, Vivero MP, Uller W, Rab R, Bovee JV, et al. Lymphatic and other vascular malformation/overgrowth disorders are caused by somatic mutations in *PIK3CA*. *J Pediatr*. 2015;166:1048–54. <https://doi.org/10.1016/j.jpeds.2014.12.069>. e1–5.
7. Kuentz P, St-Onge J, Duffourd Y, Courcet JB, Carmignac V, Jouan T, et al. Molecular diagnosis of *PIK3CA*-related overgrowth spectrum (PROS) in 162 patients and recommendations for genetic testing. *Genet Med*. 2017;19:989–97. <https://doi.org/10.1038/gim.2016.220>.
8. Brouillard P, Schlögel MJ, Homayun Sepehr N, Helaers R, Queisser A, Fastré E, et al. Non-hotspot *PIK3CA* mutations are more frequent in CLOVES than in common or combined lymphatic malformations. *Orphanet J Rare Dis*. 2021;16:267. <https://doi.org/10.1186/s13023-021-01898-y>.
9. Nozawa A, Fujino A, Yuzuriha S, Suenobu S, Kato A, Shimizu F, et al. Comprehensive targeted next-generation sequencing in patients with slow-flow vascular malformations. *J Hum Genet*. 2022;67:721–8. <https://doi.org/10.1038/s10038-022-01081-6>.
10. Samuels Y, Velculescu VE. Oncogenic mutations of *PIK3CA* in human cancers. *Cell Cycle*. 2004;3:1221–4. <https://doi.org/10.4161/cc.3.10.1164>.
11. Graupera M, Guillermet-Guibert J, Foukas LC, Phng LK, Cain RJ, Salpekar A, et al. Angiogenesis selectively requires the p110α isoform of PI3K to control endothelial cell migration. *Nature*. 2008;453:662–6. <https://doi.org/10.1038/nature06892>.
12. Castillo SD, Baselga E, Graupera M. *PIK3CA* mutations in vascular malformations. *Curr Opin Hematol*. 2019;26:170–8. <https://doi.org/10.1097/MOH.0000000000000496>.
13. Stanczuk L, Martinez-Corral I, Ulvmar MH, Zhang Y, Lavina B, Fruttiger M, et al. cKit lineage hemogenic endothelium-derived cells contribute to mesenteric lymphatic vessels. *Cell Rep*. 2015;10:1708–21. <https://doi.org/10.1016/j.celrep.2015.02.026>.
14. Brouillard P, Boon L, Vikkula M. Genetics of lymphatic anomalies. *J Clin Invest*. 2014;124:898–904. <https://doi.org/10.1172/JCI71614>.
15. Vahidnezhad H, Youssefian L, Uitto J. Molecular genetics of the PI3K-AKT-mTOR pathway in genodermatoses: diagnostic implications and treatment opportunities. *J Invest Dermatol*. 2016;136:15–23. <https://doi.org/10.1038/JID.2015.331>.
16. Samuels Y, Wang Z, Bardelli A, Silliman N, Ptak J, Szabo S, et al. High frequency of mutations of the *PIK3CA* gene in human cancers. *Science*. 2004;304:554. <https://doi.org/10.1126/science.1096502>.
17. Madsen RR, Vanhaesebroeck B, Semple RK. Cancer-associated *PIK3CA* mutations in overgrowth disorders. *Trends Mol Med*. 2018;24. <https://doi.org/10.1016/j.molmed.2018.08.003>. :856 – 70.
18. McDonough SJ, Bhagwate A, Sun Z, Wang C, Zschunke M, Gorman JA, et al. Use of FFPE-derived DNA in next generation sequencing: DNA extraction methods. *PLoS ONE*. 2019;14:e0211400. <https://doi.org/10.1371/journal.pone.0211400>.
19. Do H, Dobrovic A. Sequence artifacts in DNA from formalin-fixed tissues: causes and strategies for minimization. *Clin Chem*. 2015;61:64–71. <https://doi.org/10.1373/clinchem.2014.223040>.
20. Quindipan C, Cotter JA, Ji J, Mitchell WG, Moke DJ, Navid F, et al. Custom pediatric oncology next-generation sequencing panel identifies somatic mosaicism in archival tissue and enhances targeted clinical care. *Pediatr Neurol*. 2020;114:55–9. <https://doi.org/10.1016/j.pediatrneurol.2020.09.015>.
21. Ishikawa K, Yamamoto Y, Yamamoto Y, Furukawa H, Hayashi T, Murao N, et al. Squamous cell carcinoma arising in a chronic leg ulcer in Klippel-Trenaunay syndrome after the Charles procedure: a case with 40 years of follow up. *J Dermatol*. 2019;46:e403–e5. <https://doi.org/10.1111/1346-8138.15001>.
22. Ishikawa K, Yamamoto Y, Funayama E, Furukawa H, Sasaki S. Wound-healing problems associated with combined vascular malformations in Klippel-Trenaunay syndrome. *Adv Wound Care (New Rochelle)*. 2019;8:246–55. <https://doi.org/10.1089/wound.2018.0835>.
23. Saito N, Sasaki S, Shimizu T, Nagao M, Fujita M, Nishioka N, et al. [Venous malformations of the lower limb: a review of 110 cases]. *Japanese J Plast Surg*. 2015;58:679–86. In Japanese.
24. Lindhurst MJ, Parker VE, Payne F, Sapp JC, Rudge S, Harris J, et al. Mosaic overgrowth with fibroadipose hyperplasia is caused by somatic activating mutations in *PIK3CA*. *Nat Genet*. 2012;44:928–33. <https://doi.org/10.1038/ng.2332>.
25. Rivière JB, Mirzaa GM, O’Roak BJ, Beddaoui M, Alcántara D, Conway RL, et al. De novo germline and postzygotic mutations in *AKT3*, *PIK3R2* and *PIK3CA* cause a spectrum of related megalencephaly syndromes. *Nat Genet*. 2012;44:934–40. <https://doi.org/10.1038/ng.2331>.
26. Rios JJ, Paria N, Burns DK, Israel BA, Cornelia R, Wise CA, et al. Somatic gain-of-function mutations in *PIK3CA* in patients with macrodactyly. *Hum Mol Genet*. 2013;22:444–51. <https://doi.org/10.1093/hmg/dds440>.
27. Keppler-Noreuil KM, Sapp JC, Lindhurst MJ, Parker VE, Blumhorst C, Darling T, et al. Clinical delineation and natural history of the *PIK3CA*-related overgrowth spectrum. *Am J Med Genet Part A*. 2014;164A:1713–33. <https://doi.org/10.1002/ajmg.a.36552>.
28. MacLellan RA, Luks VL, Vivero MP, Mulliken JB, Zurakowski D, Padwa BL, et al. *PIK3CA* activating mutations in facial infiltrating lipomatosis. *Plast Reconstr Surg*. 2014;133:12e–9. <https://doi.org/10.1097/01.prs.0000436822.26709.7c>. e.
29. Loconte DC, Grossi V, Bozzao C, Forte G, Bagnulo R, Stella A, et al. Molecular and functional characterization of three different postzygotic mutations in *PIK3CA*-related overgrowth spectrum (PROS) patients: Effects on PI3K/AKT/mTOR signaling and sensitivity to PIK3 inhibitors. *PLoS ONE*. 2015;10:e0123092. <https://doi.org/10.1371/journal.pone.0123092>.
30. Mirzaa G, Timms AE, Conti V, Boyle EA, Girisha KM, Martin B, et al. *PIK3CA*-associated developmental disorders exhibit distinct classes of mutations with variable expression and tissue distribution. *JCI Insight*. 2016;1. <https://doi.org/10.1172/jci.insight.87623>.
31. Chang F, Liu L, Fang E, Zhang G, Chen T, Cao K, et al. Molecular diagnosis of mosaic overgrowth syndromes using a custom-designed next-generation sequencing panel. *J Mol Diagn*. 2017;19:613–24. <https://doi.org/10.1016/j.jmoldx.2017.04.006>.
32. Huchtagowder V, Shenoy A, Corliss M, Vigh-Conrad KA, Storer C, Grange DK, et al. Utility of clinical high-depth next generation sequencing for somatic variant detection in the *PIK3CA*-related overgrowth spectrum. *Clin Genet*. 2017;91:79–85. <https://doi.org/10.1111/cge.12819>.
33. Leiter SM, Parker VER, Welters A, Knox R, Rocha N, Clark G, et al. Hypoinsulinaemic, hypoketotic hypoglycaemia due to mosaic genetic activation of PI3-kinase. *Eur J Endocrinol*. 2017;177:175–86. <https://doi.org/10.1530/EJE-17-0132>.
34. Yeung KS, Ip JJ, Chow CP, Kuong EY, Tam PK, Chan GC, et al. Somatic *PIK3CA* mutations in seven patients with *PIK3CA*-related overgrowth spectrum. *Am J Med Genet Part A*. 2017;173:978–84. <https://doi.org/10.1002/ajmg.a.38105>.
35. Michel ME, Konczyk DJ, Yeung KS, Murillo R, Vivero MP, Hall AM, et al. Causal somatic mutations in urine DNA from persons with the CLOVES subgroup of the *PIK3CA*-related overgrowth spectrum. *Clin Genet*. 2018;93:1075–80. <https://doi.org/10.1111/cge.13195>.
36. Piacitelli AM, Jensen DM, Brandling-Bennett H, Gray MM, Batra M, Gust J, et al. Characterization of a severe case of *PIK3CA*-related overgrowth at autopsy by droplet digital polymerase chain reaction and report of *PIK3CA* sequencing in 22 patients. *Am J Med Genet Part A*. 2018;176:2301–8. <https://doi.org/10.1002/ajmg.a.40487>.
37. Siegel DH, Cottrell CE, Streicher JL, Schilter KF, Basel DG, Baselga E, et al. Analyzing the genetic spectrum of vascular anomalies with overgrowth via cancer genomics. *J Invest Dermatol*. 2018;138:957–67. <https://doi.org/10.1016/j.jid.2017.10.033>.
38. Wu J, Tian W, Tian G, Sumner K, Hutchinson DT, Ji Y. An investigation of *PIK3CA* mutations in isolated macrodactyly. *J Hand Surg Eur Vol*. 2018;43:756–60. <https://doi.org/10.1177/1753193418770366>.

39. Lalonde E, Ebrahimzadeh J, Rafferty K, Richards-Yutz J, Grant R, Toorens E, et al. Molecular diagnosis of somatic overgrowth conditions: a single-center experience. *Mol Genet Genomic Med*. 2019;7:e536. <https://doi.org/10.1002/mgg3.536>.
40. Blackburn PR, Milosevic D, Marek T, Folpe AL, Howe BM, Spinner RJ, et al. *PIK3CA* mutations in lipomatosis of nerve with or without nerve territory overgrowth. *Mod Pathol*. 2020;33:420–30. <https://doi.org/10.1038/s41379-019-0354-1>.
41. Davis S, Ware MA, Zeiger J, Deardorff MA, Grand K, Grimberg A et al. Growth hormone deficiency in megalencephaly-capillary malformation syndrome: an association with activating mutations in *PIK3CA*. *American journal of medical genetics part A*. 2020;182:162–8. <https://doi.org/10.1002/ajmg.a.61403>.
42. Le Cras TD, Goines J, Lakes N, Pastura P, Hammill AM, Adams DM, et al. Constitutively active *PIK3CA* mutations are expressed by lymphatic and vascular endothelial cells in capillary lymphatic venous malformation. *Angiogenesis*. 2020;23:425–42. <https://doi.org/10.1007/s10456-020-09722-0>.
43. Park HJ, Shin CH, Yoo WJ, Cho TJ, Kim MJ, Seong MW, et al. Detailed analysis of phenotypes and genotypes in megalencephaly-capillary malformation-polymicrogyria syndrome caused by somatic mosaicism of *PIK3CA* mutations. *Orphanet J Rare Dis*. 2020;15:205. <https://doi.org/10.1186/s13023-020-01480-y>.
44. Tian W, Huang Y, Sun L, Guo Y, Zhao S, Lin M, et al. Phenotypic and genetic spectrum of isolated macrodactyly: somatic mosaicism of *PIK3CA* and *AKT1* oncogenic variants. *Orphanet J Rare Dis*. 2020;15:288. <https://doi.org/10.1186/s13023-020-01572-9>.
45. Garde A, Guibaud L, Goldenberg A, Petit F, Dard R, Roume J, et al. Clinical and neuroimaging findings in 33 patients with MCAP syndrome: a survey to evaluate relevant endpoints for future clinical trials. *Clin Genet*. 2021;99:650–61. <https://doi.org/10.1111/cg.13918>.
46. Palmieri M, Pinto AM, di Blasio L, Curro A, Monica V, Sarno LD, et al. A pilot study of next generation sequencing-liquid biopsy on cell-free DNA as a novel non-invasive diagnostic tool for Klippel-Trenaunay syndrome. *Vascular*. 2021;29:85–91. <https://doi.org/10.1177/1708538120936421>.
47. Gökpinar İli E, Tasdelen E, Durmaz CD, Altiner S, Tuncali T, Martinez-Glez V, et al. Phenotypic and molecular characterization of five patients with *PIK3CA*-related overgrowth spectrum (PROS). *Am J Med Genet Part A*. 2022;188:1792–800. <https://doi.org/10.1002/ajmg.a.62709>.
48. Mussa A, Leoni C, Iacoviello M, Carli D, Ranieri C, Pantaleo A, et al. Genotypes and phenotypes heterogeneity in *PIK3CA*-related overgrowth spectrum and overlapping conditions: 150 novel patients and systematic review of 1007 patients with *PIK3CA* pathogenetic variants. *J Med Genet*. 2023;60:163–73. <https://doi.org/10.1136/jmedgenet-2021-108093>.
49. Boscolo E, Coma S, Luks VL, Greene AK, Klagsbrun M, Warman ML, et al. AKT hyper-phosphorylation associated with *PI3K* mutations in lymphatic endothelial cells from a patient with lymphatic malformation. *Angiogenesis*. 2015;18:151–62. <https://doi.org/10.1007/s10456-014-9453-2>.
50. Limaye N, Kangas J, Mendola A, Godfraind C, Schlögel MJ, Helaers R, et al. Somatic activating *PIK3CA* mutations cause venous malformation. *Am J Hum Genet*. 2015;97:914–21. <https://doi.org/10.1016/j.ajhg.2015.11.011>.
51. Ten Broek RW, Eijkelenboom A, van der Vleuten CJM, Kamping EJ, Kets M, Verhoeven BH, et al. Comprehensive molecular and clinicopathological analysis of vascular malformations: a study of 319 cases. *Genes Chromosomes Cancer*. 2019;58:541–50. <https://doi.org/10.1002/gcc.22739>.
52. Zenner K, Cheng CV, Jensen DM, Timms AE, Shivaram G, Bly R, et al. Genotype correlates with clinical severity in *PIK3CA*-associated lymphatic malformations. *JCI Insight*. 2019;4. <https://doi.org/10.1172/jci.insight.129884>.
53. Wang S, Wang W, Zhang X, Gui J, Zhang J, Guo Y, et al. A somatic mutation in *PIK3CD* unravels a novel candidate gene for lymphatic malformation. *Orphanet J Rare Dis*. 2021;16:208. <https://doi.org/10.1186/s13023-021-01782-9>.
54. Zenner K, Jensen DM, Cook TT, Dmyterko V, Bly RA, Ganti S, et al. Cell-free DNA as a diagnostic analyte for molecular diagnosis of vascular malformations. *Genet Med*. 2021;23:123–30. <https://doi.org/10.1038/s41436-020-00943-8>.
55. Zenner K, Jensen DM, Dmyterko V, Shivaram GM, Myers CT, Paschal CR, et al. Somatic activating *BRAF* variants cause isolated lymphatic malformations. *HGG Adv*. 2022;3:100101. <https://doi.org/10.1016/j.xhgg.2022.100101>.
56. Huang CH, Mandelker D, Schmidt-Kittler O, Samuels Y, Velculescu VE, Kinzler KW, et al. The structure of a human p110α/p85α complex elucidates the effects of oncogenic *PI3Kα* mutations. *Science*. 2007;318:1744–8. <https://doi.org/10.1126/science.1150799>.
57. Suppan C, Graf R, Jahn S, Zhou Q, Klocker EV, Bartsch R, et al. Sensitive and robust liquid biopsy-based detection of *PIK3CA* mutations in hormone-receptor-positive metastatic breast cancer patients. *Br J Cancer*. 2022;126:456–63. <https://doi.org/10.1038/s41416-021-01601-9>.
58. Hori Y, Hirose K, Aramaki-Hattori N, Suzuki S, Nakayama R, Inoue M, et al. Fibro-adipose vascular anomaly (FAVA): three case reports with an emphasis on the mammalian target of rapamycin (mTOR) pathway. *Diagn Pathol*. 2020;15:98. <https://doi.org/10.1186/s13000-020-01004-z>.
59. Uihlein LC, Liang MG, Fishman SJ, Alomari AI, Mulliken JB. Capillary-venous malformation in the lower limb. *Pediatr Dermatol*. 2013;30:541–8. <https://doi.org/10.1111/pde.12186>.
60. Couto JA, Ayturk UM, Konczyk DJ, Goss JA, Huang AY, Hann S, et al. A somatic *GNA11* mutation is associated with extremity capillary malformation and overgrowth. *Angiogenesis*. 2017;20:303–6. <https://doi.org/10.1007/s10456-016-9538-1>.
61. Limaye N, Wouters V, Uebelhoer M, Tuominen M, Wirkkala R, Mulliken JB, et al. Somatic mutations in angiopoietin receptor gene *TEK* cause solitary and multiple sporadic venous malformations. *Nat Genet*. 2009;41:118–24. <https://doi.org/10.1038/ng.272>.
62. Narayan P, Prowell TM, Gao JJ, Fernandes LL, Li E, Jiang X, et al. FDA approval summary: alpelisib plus fulvestrant for patients with HR-positive, HER2-negative, *PIK3CA*-mutated, advanced or metastatic breast cancer. *Clin Cancer Res*. 2021;27:1842–9. <https://doi.org/10.1158/1078-0432.CCR-20-3652>.
63. theascreen *PIK3CA* RGQ PCR Kit Instructions for Use (Handbook) Version 1. QIAGEN GmbH. 2019;55 – 6. <https://www.qiagen.com/us/resources/resourcedetail?id=2d7ab465-a0e2-4311-8f90-1bea278aa47e&en>. Accessed 19 Dec 2022.
64. Hammer J, Seront E, Duez S, Dupont S, Van Damme A, Schmitz S, et al. Sirolimus is efficacious in treatment for extensive and/or complex slow-flow vascular malformations: a monocentric prospective phase II study. *Orphanet J Rare Dis*. 2018;13:191. <https://doi.org/10.1186/s13023-018-0934-z>.
65. Parker VER, Keppler-Noreuil KM, Faviere L, Luu M, Oden NL, De Silva L, et al. Safety and efficacy of low-dose sirolimus in the *PIK3CA*-related overgrowth spectrum. *Genet Med*. 2019;21:1189–98. <https://doi.org/10.1038/s41436-018-0297-9>.
66. Forde K, Resta N, Ranieri C, Rea D, Kubassova O, Hinton M, et al. Clinical experience with the AKT1 inhibitor miransertib in two children with *PIK3CA*-related overgrowth syndrome. *Orphanet J Rare Dis*. 2021;16:109. <https://doi.org/10.1186/s13023-021-01745-0>.
67. Venot Q, Blanc T, Rabia SH, Berteloot L, Ladraa S, Duong JP, et al. Targeted therapy in patients with *PIK3CA*-related overgrowth syndrome. *Nature*. 2018;558:540–6. <https://doi.org/10.1038/s41586-018-0217-9>.
68. Luu M, Vabres P, Devilliers H, Loffroy R, Phan A, Martin L, et al. Safety and efficacy of low-dose *PI3K* inhibitor taselisib in adult patients with CLOVES and Klippel-Trenaunay syndrome (KTS): the TOTEM trial, a phase 1/2 multicenter, open-label, single-arm study. *Genet Med*. 2021;23:2433–42. <https://doi.org/10.1038/s41436-021-01290-y>.
69. Canaud G, Hammill AM, Adams D, Vikkula M, Keppler-Noreuil KM. A review of mechanisms of disease across *PIK3CA*-related disorders with vascular manifestations. *Orphanet J Rare Dis*. 2021;16:306. <https://doi.org/10.1186/s13023-021-01929-8>.
70. Maari C, Frieden IJ. Klippel-Trenaunay syndrome: the importance of geographic stains in identifying lymphatic disease and risk of complications. *J Am Acad Dermatol*. 2004;51:391–8. <https://doi.org/10.1016/j.jaad.2003.12.017>.
71. Funayama E, Sasaki S, Oyama A, Furukawa H, Hayashi T, Yamamoto Y. How do the type and location of a vascular malformation influence growth in Klippel-Trenaunay syndrome? *Plast Reconstr Surg*. 2011;127:340–6. <https://doi.org/10.1097/PRS.0b013e3181f95b4c>.
72. Enjolras O, Wassef M, Chapot R. Venous malformations (VM). *Color Atlas of vascular tumors and vascular malformations*, 168–223, Cambridge University Press, New York, 2007.

Publisher's Note

Springer Nature remains neutral with regard to jurisdictional claims in published maps and institutional affiliations.